

COMBINATION OF DISTANCE DATA WITH HIGH RESOLUTION IMAGES

R. Reulke

^a HU-Berlin, Computer Vision, 10099 Berlin, Germany- reulke@informatik.hu-berlin.de

Commission V, WG V/5

KEY WORDS: *Vision, Fusion, Camera, Scanner, DEM/DTM, Orthorectification*

ABSTRACT:

Typical devices for acquiring distance data are laser scanners. Combining these with higher resolution image data is state of the art. Recently, camera systems are available providing distance and image data without usage of mechanical parts. Two manufacturers of such camera systems with a typical resolution of 160 x 120 pixels are CSEM Swiss Ranger and PMDTechnologies GmbH. This paper describes a design, combining a PMD and a higher resolution RGB camera. For error-free operation, calibration of both cameras and alignment determination between both systems is necessary. This way, a performance determination of the PMD system is also possible.

1. INTRODUCTION AND MOTIVATION

The fusion of high resolution camera with laser scanner data is a promising approach and allows the combination of high-resolution image and depth data. Application areas are indoor building modelling, computer vision and documentation of cultural heritage (Reulke, 2005).

Recent methods offer 3D animated videos or interactive 3D models for 3D scene visualization. The acquisition of additional range data is crucial for creating 3D models and different alternatives are provided in close-range photogrammetry.

For modelling a 3D scene, image or distance based approaches are possible. Distance related scene modelling based on laser scanner data has been used for close-range photogrammetry (e.g., acquisition of building geometries) for several years. An overview of actual available laser scanner systems can be found in (Wehr 2005).

Many projects require high resolution true-colour surface textures. There are several combined systems which provide the option of additional colour data capturing. This is solved by mounting a camera near the laser diode or by complex mechanical mirror systems. Most systems use additional commercial CCD frame cameras.

Recently small and compact imaging systems with distance measurement capability are available.

The present article describes the combination of a higher camera and a PMD-system. Two manufacturers of such camera systems with a typical resolution of 160 x 120 pixels are CSEM Swiss Ranger and PMDTechnologies GmbH.

The paper is organized as follows: In the second chapter the PMD-system will be described and in the following the system will be analysed. The fourth chapter describes the results of fusion with higher resolution image data.

2. PMD – CAMERA

2.1 PMD - Principle

A Photonic Mixer Device (PMD) allows capturing the complete 3D scene (distance and gray value) in real time. The approach is equivalent to laser scanner. A summary of different distance measure principles for laser scanner can be found in (Wehr,

2005). There are different ranging principles applied in terrestrial laser scanning. In terrestrial laser scanning ranging is carried out either by triangulation or by measuring the time of flight of the laser signal. For the time-of-flight measurements, short pulses with high peak power are produced by lasers. The travelling time of a laser pulse is measured. Another possibility to determine the travelling time of a signal is realized by measuring the phase difference between the transmitted and received signal.

In continuous wave (cw) laser ranging the laser intensity is modulated with a well defined function e.g. a sinusoidal or a square wave signal. The modulation signal is repeated continuously. The time of flight of the signal is determined by measuring the phase difference between the transmitted and the received signal. The period time T_{pd} , the frequency f or wavelength λ defines the maximum unambiguous range r_{un} , which is $\lambda/2$ for two-way ranging.

To obtain 3D information of the entire scene, a modulated single laser beam would have to be scanned mechanically over the scene.

In PMD each pixel can individually measure phase shift of the modulated light. This is done by using continuous square wave modulation and measuring the phase delay for each pixel. A special advantage of PMD is that the complete mixing process of the electric and optical signal takes place within each pixel.

Detector pixel dimension	40 μ m x 40 μ m
# pixel (v,h)	160 (h) x 120 (v)
Optics adapter	C-mount
Modulation frequency	20 MHz (7.5 m ambiguity interval)
FOV	40° @f=12 mm
Wavelength	870 nm
Interface	FireWire, Ethernet
Weight	1400g

Table 1. Specification for PMD [vision]® 19k

A modulated optical signal sent by a transmitter (near infrared light source at $\lambda = 850$ nm), illuminates the scene to be measured. The reflected light enters the PMD sensor, which is also connected to the modulation source. The charges in the p-type semiconductor, generated by the photons, are separated

inside the optically sensitive area of the semiconductor in relation to the reference signal. The resulting output signal depends on the phase shift of the reflected optical signal (which carries the desired 3D information) and the electrical modulation signals for the illumination source in the chip. Table 1 gives an overview of the performance of the sensor.

2.2 PMD Camera Calibration

By using PMD measurements, distance information for each pixel is available. On the other hand the spatial coordinates are necessary. A relation for deriving coordinate information from this distance information can be derived. Figure 1 shows the geometry:

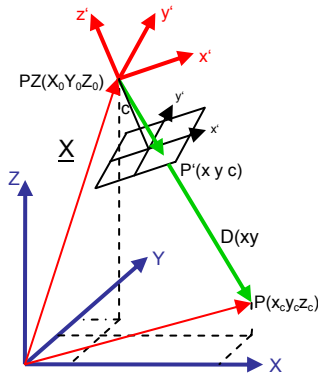


Figure 1: Geometric relation for PMD

The coordinate measurement is related to the projection centre (PZ) of the PMD-camera. Therefore the camera position and the view direction, which are equivalent to the exterior orientation are fixed in $X_0=0, Y_0=0, Z_0=0$ and $\omega=0, \varphi=0, \kappa=0$. For a pixel with the coordinates (x, y) a distance $d(x, y)$ was measured. The object coordinates (x_c, y_c, z_c) in the PMD frame can be calculated as follows:

$$z_c = d(x, y) \cdot \frac{c}{\sqrt{c^2 + x^2 + y^2}} \quad x_c = x \cdot \frac{r_{xy}}{\sqrt{x^2 + y^2}} \quad y_c = y \cdot \frac{r_{xy}}{\sqrt{x^2 + y^2}}$$

with

$$r_{xy} = \sqrt{d^2 - z^2} \quad (1)$$

(x, y) are the image coordinates in the PMD camera frame but the measurement is related to rows and columns. To determine the image coordinates, principle point, focal length and additional distortion effects have to be corrected. This is a typical problem of camera calibration or interior orientation determination in photogrammetric sense.

The determination of interior and exterior orientation is based on the collinearity equations. The collinearity equation describes the geometry between the sensors projection centre, the coordinates of an object and the image coordinates in relation to the principle point. Figure 1 shows the geometric relation between projection centre, object points and image coordinates. To transform object coordinates to image coordinates, the following relation can be used:

$$x' = x'_0 - c \cdot \frac{r_{11} \cdot (X - X_0) + r_{12} \cdot (Y - Y_0) + r_{13} \cdot (Z - Z_0)}{r_{31} \cdot (X - X_0) + r_{32} \cdot (Y - Y_0) + r_{33} \cdot (Z - Z_0)} \quad (2)$$

$$y' = y'_0 - c \cdot \frac{r_{21} \cdot (X - X_0) + r_{22} \cdot (Y - Y_0) + r_{23} \cdot (Z - Z_0)}{r_{31} \cdot (X - X_0) + r_{32} \cdot (Y - Y_0) + r_{33} \cdot (Z - Z_0)}$$

where X, Y, Z = Object coordinates
 x', y' = Image coordinates
 x'_0, y'_0, c = Principle point, focal length
 X_0, Y_0, Z_0 = Projection centre

$$\underline{\underline{R}}(\omega, \varphi, \kappa) = \begin{pmatrix} r_{11} & r_{12} & r_{13} \\ r_{21} & r_{22} & r_{23} \\ r_{31} & r_{32} & r_{33} \end{pmatrix} \quad \text{Matrix for rotation into the image coordinate system}$$

A standard reference for interior orientation is the Brown model (Brown, 1971) which is implemented in the Australis bundle block adjustment program (Fraser, 2000). The image coordinate correction function in Australis is the commonly used 10-parameter model. The calibration parameters can be grouped as follows:

- Camera interior orientation: c, x_0, y_0
- Radial distortion parameters: k_1, k_2, k_3
- Decentering distortion parameters: p_1, p_2
- Affinity, non-orthogonality parameters: b_1, b_2

The corrected image coordinates (x_{corr}, y_{corr}) can be calculated from the measured coordinates (x_{meas}, y_{meas}) using the formulas

$$x = x_{meas} - x_0 \quad y = y_{meas} - y_0$$

$$r^2 = x^2 + y^2 \quad (3)$$

$$x_{corr} = x_{meas} - x_0 + \Delta x = x + \Delta x$$

$$y_{corr} = y_{meas} - y_0 + \Delta y = y + \Delta y$$

Δx and Δy represent the corrections due to the described effects. The PMD-camera was calibrated with Australis. The imaging mode of the PMD-camera gives poor image quality; therefore an additional CCD-camera was used, to identify the image structures in the PMD image. The camera is a DBK 41BF02 with 1280 x 960 pixel, which realizes colour with Bayer mosaic (see web site from TheImagingSource).

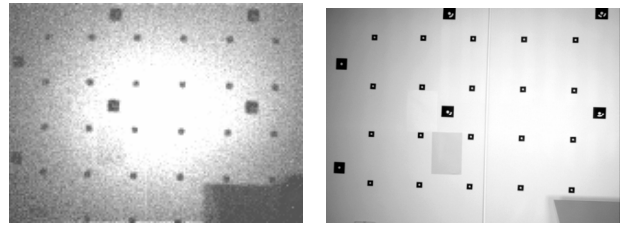


Figure 2 Greyscale image of PMD-camera (left) and DBK-camera (right)

For comparison figure 2 shows the image of the PMD-camera and an image from the DBK-camera. The strong signal change in the PMD-image is related to the own illumination system of the PMD-system. An additional speckle noise is also visible. The labels shown in the image are also used for calibration. The focal length of both systems is about 12 mm. In spite of the fact that the number of pixel differs roughly by a factor of 8, the image of the object is nearly the same. The reason is that the pixel size differs by the same relation (40 μ m pixel distance for PMD to 5 μ m for the DBK).

Parameter	DBK	PMD
Sensor_Size_H	1280	160
Sensor_Size_V	960	120

Pixel_Size_H	0.005	0.04
Pixel_Size_V	0.005	0.04
C	13.5895	11.9926
XP	0.2717	-0.0406
YP	0.1387	0.1839
K1	6.30411e-004	3.30242e-003
K2	2.84142e-006	-2.84237e-004
K3	-2.98286e-007	2.09350e-005
P1	-6.10220e-005	2.11975e-004
P2	8.09806e-005	2.64842e-004
B1	-2.10203e-004	8.13613e-005
B2	2.07497e-005	-1.51093e-004

Table 2. Result of the calibration of PMD and DBK, parameters are in [mm]

Table 2 gives the result of the calibration of both cameras. Particularly with regard to principle point and distortion, significant influence is visible.

The accuracy of the calibration can be measured with the standard deviation of the block adjustment σ_0 , which is in the range of 1/10 of a pixel distance for DBK-camera and 1/4 of a pixel for the PMD-camera. The reason for the unsatisfactory calibration result of the PMD-camera is the accuracy of point determination in the PMD-images.

The known interior orientation now allows the determination of the exterior orientation from known object points e.g. with spatial resection algorithm. Spatial Resection is a widely used tool in photogrammetry for nonlinear calculation of the exterior orientation from more than three targets with known coordinates.

3. INVESTIGATION OF PMD DATA

3.1 Reproducibility and accuracy calculation

The determination of the object coordinates (x_c, y_c, z_c) in the PMD frame can be obtained with the help of the known interior orientation and by using equations (1).

The accuracy determination means the precision and the standard deviation for distance measurement and was done with a plane surface in front of the PMD-camera, as shown in figure 2. A plane is described by a point $P_0(x_0, y_0, z_0)$ and the direction cosines (a, b, c) of the normal to the plane as follows (see also Luhmann, 2003):

$$0 = a \cdot (x_i - x_0) + b \cdot (y_i - y_0) + c \cdot (z_i - z_0) \quad (4)$$

The distance from any point $Q(x_i, y_i, z_i)$ to a plane specified above is given by

$$d_i = a \cdot (x_i - x_0) + b \cdot (y_i - y_0) + c \cdot (z_i - z_0) \quad (5)$$

The sum of squares of distances of each point from the plane is

$$F = \sum_{i=1}^n d_i^2 \quad (6)$$

By using the optimal parameters (a,b,c), F is minimised. The best-fit plane passes through (x_0, y_0, z_0) , which is the average of the data points. The direction cosines (a,b,c) can be obtained by

using the eigenvector associated with the smallest eigenvalue of the matrix

$$\underline{\underline{B}} = \underline{\underline{A}}^T \cdot \underline{\underline{A}} \quad (7)$$

The matrix A is formulated such that three column are $[x_i - x_0, y_i - y_0, z_i - z_0]$ (Forbes, 1989). Mean and standard deviation of d_i gives general information about reproducibility and accuracy of the PMD-device.

No	z0	a	b	c	$\langle d_i^2 \rangle$
0	4152.02	-0.0652	-0.0108	0.9978	78.53
1	4152.52	-0.0663	-0.0052	0.9978	82.59
2	4152.22	-0.0619	-0.0108	0.9980	64.31
3	4155.45	-0.0620	-0.0088	0.9980	71.34
4	4150.73	-0.0659	-0.0088	0.9978	74.08
5	4147.31	-0.0669	-0.0072	0.9977	74.93
6	4150.18	-0.0633	-0.0096	0.9980	77.39
7	4138.40	-0.0661	-0.0075	0.9978	74.25
8	4142.84	-0.0679	-0.0090	0.9977	70.36
9	4146.49	-0.0654	-0.0101	0.9978	83.21

Table 3. Accuracy of PMD distances measurement with integration time of 10 ms.

This result shows a large standard deviation of 75 mm. The reason is the large differences in reflection properties of the markers. Following figure shows a surface view of the distance data with an image overlay.

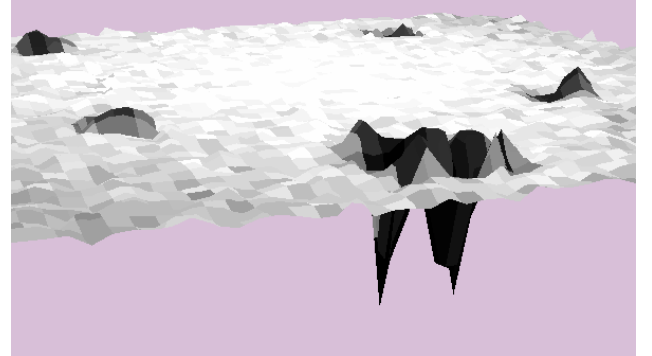


Figure 3: Distance error due to changing reflection properties. A texturised surface view.

Several algorithms are investigated to filter the distance errors due to strong reflection changes and to find out optimal distance values. In a window of $(2m+1, 2m+1)$ the reflected amplitudes are analysed. If the amplitude is larger than a value c, the distance value will be used for further evaluation. The corrected distance at pixel (i, j) can be evaluated from the remaining distance values by median or mean filter.

$$\bar{d}_{i,j} = \begin{cases} d_{i,j} & \text{if } a_{i,j} > c \\ \emptyset & \text{if } a_{i,j} \leq c \end{cases} \quad (i,j) \in [-m, m] \quad (8)$$

$$d_{i,j}^{corr} = \langle \bar{d}_{i,j} \rangle$$

The standard deviation calculated from median is 17.5 mm and from mean with 11 mm. For the following calculation the mean is used. This is equivalent to an accuracy of about 2.5 ‰ (for an integration time of 10 ms) in relation to the object distance.

The integration time has a strong influence to the accuracy. Experimental results (see table 4) shows, that the integration time should be in a range between 5 ms and 50 ms. Lower values then 5 ms are inaccurate because of noise and poor reflected intensity. With higher integration (> 50 ms) time saturation effect can be seen. It seems, that distance measure depends from the integration time.

Frame	integration time [ms]	Distance [mm]	standard deviation [mm]	standard deviation/distance [%]
1	2	4210.92	71.65	17.02
2	5	4177.98	13.74	3.29
3	10	4161.90	5.13	1.23
4	20	4124.76	4.39	1.06
5	50	4109.64	3.67	0.89
6	100	4137.52	25.31	6.12

Table 4. Accuracy of PMD distances measurement with varying integration time of 10 ms. (The distance is 4192 mm measured with a handheld laser rangefinder.)

The absolute accuracy was compared with a handheld laser rangefinder and is in the range of 50 mm. An accurate comparison with derived data from photogrammetric approaches gives the same result. Table 5 shows the result for different distances to a flat wall.

Frame	Measured distance [mm]	PMD distance [mm]	Standard deviation [mm]
1	4000	3961.68	1.64
2	5351	5317.22	2.34
3	7292	7258.73	3.45
4	7292	7269.80	2.99
7	11540	4032.95	6.80

Table 5. Accuracy of distance measurement (integration time 50 ms) in comparison with a handheld laser rangefinder.

For a larger distance than the maximum unambiguous range r_{un} the observed value is modulo r_{un} ($=7.5$ m). The standard derivation however is equivalent to 11.5 m and can be used as a tool to overcome ambiguities.

The standard deviation for PMD distance measurement is about 0.5-1 %, the reproducibility is less than 0.5% and the absolute accuracy is about 1%.

4. FUSION WITH HIGH RESOLUTION IMAGES

For tests a small object (cat) of a size less than 1 m was used.

4.1 Co-alignment of different cameras frames

The determination of the relative orientation of both cameras seems to be not accurate enough because of weak mechanical stability between the cameras. Therefore object coordinates derived from PMD distance image are transformed into the lab coordinate frame. Each image from other cameras with known exterior and interior orientation can be used for combination with PMD data. The relation between Lab and PMD coordinate system is:

$$\underline{x}^{PMD} = \underline{R}_{Lab}^{PMD} + \underline{x}_{Lab}^{PMD} \quad (9)$$

As seen in figure 4 the transformation can be derived from the exterior orientation of the PMD-camera, which is equivalent to the transformation from the camera coordinate system into the world coordinate system:

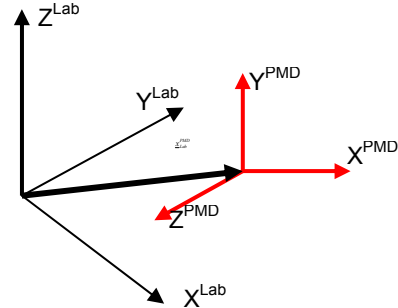


Figure 4: PMD and Lab-coordinate systems

An additional rotation of 180° around the z-axis may be necessary, if the internal coordinate system starts on the upper left site.

4.2 Derivation of a DHM

For each pixel in the PMD data set, the x, y and z coordinates can be derived. Because of the lens distortion the derived DHM is not equidistant in x- and y-direction. An additional resampling algorithm (gridding) of the (x, y, z) data on a regular grid is necessary. Different approaches and programs are available and implemented. Here, an ENVI toolbox was used. Figure 9 shows the processed PMD data for DHM and the image.

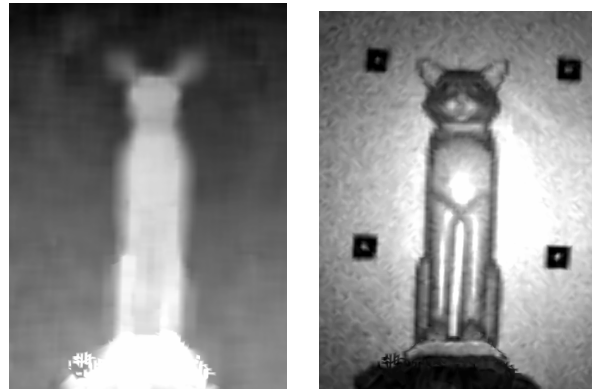


Figure 5. DHM (left) and image (right) of the object after gridding

The same object was recorded with the higher resolution DBK-camera. The mapping of the high resolution texture on the low resolution DHM is equivalent to the orthophoto generation. The known procedure (Luhmann, 2003) can be realized in three steps:

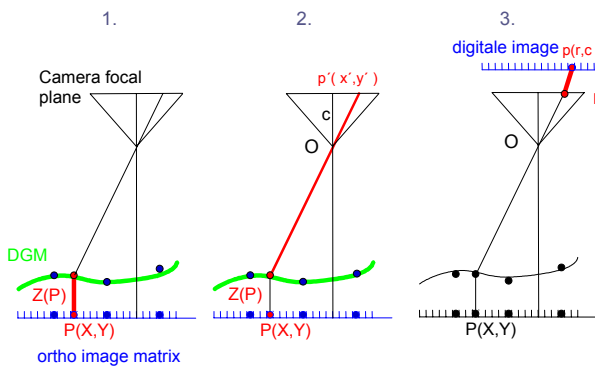


Figure 6. Orthophoto generation

1. Define ortho-image size and pixel size. For an object point $P(X,Y)$, the equivalent Z -value can be determined by interpolation of the gridded DHM data, which is in the Lab coordinate system.
2. With the collinearity equation the image point can be calculated. The exterior orientation of the camera has to be determined before.
3. Using the interior orientation model, the image point (in rows and columns) can be determined. The grey value from this image point has to be used with the ortho-image matrix.

The Brown model however was designed to calculate the corrected pixel from measured pixel position. Therefore an inverse procedure is necessary, which can iteratively calculate the uncorrected pixel position from corrected one. As a result an ortho-corrected image with higher resolution in comparison to the DHM resolution can be derived. The following figure shows the ortho-image and texture DHM.

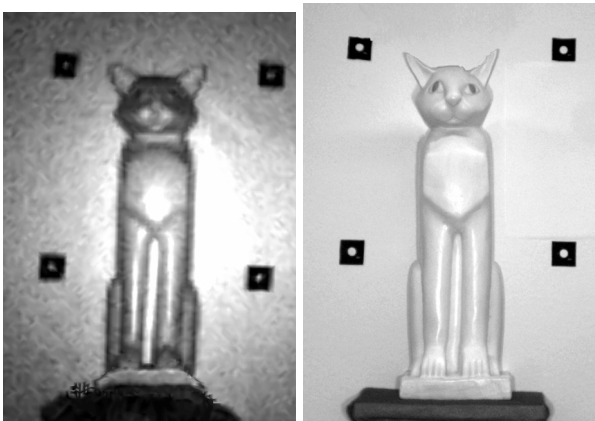


Figure 7. Result of the orthophoto generation. PMD image (left), rectified DBK image (right)

Figure 8 shows the texturized DHM from the object.

5. CONCLUSION AND OUTLOOK

The present paper investigates an imaging system with distance measuring capability. An approach for combining distance and higher resolution image data was presented. This is a prerequisite e.g. for real time 3D imaging.

The accuracy of the described procedure needs further investigation.



Figure 8. A texturized DHM

References from Journals:

- Brown, D.C., 1971. Photometric Engineering, pages 855-866, Vol. 37, No. 8.
- Fraser, C. S. , Edmundson, K. L. 2000. Design and Implementation of a Computational Processing System for Off-Line Digital Close-Range Photogrammetry, ISPRS Journal of Photogrammetry & Remote Sensing, 55(2): 94-104.
- Reulke, R., Scheibe, K., Wehr, A., 2005. Integration of digital panoramic camera and laser scanner data, International Workshop on Recording, Modeling and Visualization of Cultural Heritage, Ascona.
- Schwarte R., 1997. A new electrooptical mixing correlation sensor: Facilities and Applications of the Photonic Mixer Device (PMD), Proc. SPIE Vol. 3100, 245-253.
- Wehr, A. 2005. Laser Scanning and Its Potential to Support 3D Panoramic Recording, IAPRS, VOLUME XXXVI-5/W8, Editors: R. Reulke, U. Knauer
- Xu, Z. , Schwarte, R. , Heinol, H. , Buxbaum, B. , Ringbeck, T., Smart pixel - photonic mixer device (PMD), New system concept of a 3D-imaging camera-on-a-chip.

References from Books:

- Luhmann, T. Nahbereichsphotogrammetrie, 2. Auflage, Wichmann Verlag, 2003

References from Other Literature:

- Forbes, A.B., Least-square best-fit geometric elements. National Physical Laboratory, Report DITC 140/89, Teddington, United Kingdom.

References from websites:

- TheImagingSource:
http://www.1394imaging.com/de/products/cameras/firewire_bayer/dbk41bf02/overview/

- Australis: www.photometrix.com.au